Advanced nanocrystalline ZrO_2 for optical oxygen sensors

Janusz D. Fidelus and Witold Łojkowski
Laboratory of Nanostructures
Institute of High Pressure Physics, Polish Acad. of Sciences
Warsaw, Poland
e-mail: jdf@unipress.waw.pl

Donats Millers, Krisjanis Smits and Larisa Grigorjeva
Division of Disordered Material Physics
Institute of Solid State Physics
Riga, Latvia
e-mail: dmillers@latnet.lv

Abstract **It was shown that ZrO_2 nanopowders and nanoceramics can be used as an optical oxygen sensor, where the luminescence signal is proportional to the partial oxygen pressure in gases. The nanopowders were obtained in a hydrothermal microwave driven process followed by annealing at 750°C. Nanoceramics were obtained by sintering at pressures up to 6 GPa and at 250°C so that grain growth did not occur. Luminescence of both materials depends linearly on the oxygen content in nitrogen-oxygen mixtures for 2.1% - 25 vol% oxygen content. For luminescence excitation using a laser beam, the luminescence intensity decreases as oxygen pressure increases. For excitation with an electron beam, the opposite effect is observed – the lower the oxygen pressure, the lower the luminescence signal. The experimental results are explained in terms of luminescence centers being distorted lattice sites close to vacancies.**

I. Introduction

Optical oxygen pressure sensors based on the phenomenon of change of luminescence intensity of organic materials are well known. However, these sensors are costly and their upper temperature operation limit is 80ºC. Therefore developing of an inorganic material with luminescence properties depending on oxygen pressure is of high practical and scientifical interest. ZrO_2 is a material having a large number of applications [1-5], and is also used in electrical sensors for oxygen pressure detection [6]. The operation of these sensors is based on oxygen ions transport in which oxygen vacancies are involved. On the other hand, vacancies may contribute to luminescence of ZrO_2 because of the possibility to attract self-trapped excitons and their possible contribution to lattice distortions [7-12]. At room temperature only luminescence of lattice (intrinsic) defects is observed because luminescence of self-trapped excitons is thermally quenched above 150 K [7]. Since the concentration of oxygen vacancies may depend on oxygen pressure above the sample, luminescence of this material may depend on oxygen pressure as well. In fact, we recently discovered the dependence of luminescence intensity in zirconia nanoparticles on oxygen partial pressure and suggested the application of the effect in oxygen sensors [13 -17].

In the present paper we show further results confirming the possibility to use ZrO_2 nanoparticles and nanoceramics in optical oxygen sensors that may have alternative applications comparing to the well known dye-containing membrane sensors or electrical sensors. We discuss also the possible mechanism for the dependence of luminescence on oxygen pressure.

This work was supported by Ministry of Science and Higher Education (Poland), (grant no. N N508 0851 33 and "DONANO") as well as by the Latvian State Material Research Programme and Latvian Council of Science (grant 05.0026.)

II. Experimental

A. Samples

The ZrO_2 nanopowder was obtained by hydrothermal microwave driven process (MW), described in details in [14,15], and then heated in air up to 750 °C at a rate of 15 °C min^{-1}, held at this temperature for 30 min and subsequently cooled down. This thermal treatment permits to obtain particles of the monoclinic phase and grain size stable at 340 °C, i.e., at the temperature at which the samples in sensor material tests were annealed under variable oxygen pressure. The ZrO_2 nanostructured ceramics was obtained by sintering the ZrO_2 nanopowder using the high pressure – low temperature sintering (HPLS) process. The pellets of 5 mm diameter and 2 mm thickness were formed under toroidal press at 6 GPa and sintered at 250 ºC for 1 min.

B. Structural Properties

X-ray diffraction (XRD) patterns of MW ZrO_2 nanopowder as well as HPLS ZrO_2 ceramics were collected in the 2θ range of 10 – 100° at room temperature, with a step of 0.05° using a D5000 (Siemens) X-ray diffractometer with $CuK_{\alpha 1}$ radiation. The average grain sizes determined by XRD using the Scherrer equation were 31 nm and 27 nm for nanopowder and ceramics, respectively. The Grain Size Distribution (GSD) was determined using the method of XRD peak fine structure analysis (XRD-GSD) [15]. This method permits fitting the XRD peaks using an analytical function and determine the average particle diameter <R> and dispersion of particle sizes <s>. The samples morphology was determined using a LEO 1530 field emission scanning microscope. The

density of the nanopowders was measured by means of helium picnometry using a AccuPyc 1330, produced by Micrometrics Instruments. The specific surface area analysis was determined by the multipoint B.E.T. method (Gemini 2360, Micromeritics Instruments).

C. Annealing in mixed Oxygen and Nitrogen atmospheres

Both, MW ZrO_2 nanopowder and HPLS ZrO_2 ceramics were loaded into quartz tube from which the air was evacuated. The tube was filled with mixtures of oxygen and nitrogen (1 atm. pressure) with different O_2 contents (from 2.1% to 23.4%) or in vacuum (10^{-4} mbar) and heated up to 340 °C and held at this temperature for 20 minutes and then cooled to room temperature and opened. The individual stages of material treatment are described in details in [14].

D. Luminescence Measurements

For luminescence investigations the nanopowders were pressed into pellets. Most investigations were carried out at room temperature and in air. One series of tests using electron beam excitation was carried out in real time during heating and cooling. Two luminescence excitation methods were used: illumination with pulsed YAG:Nd laser beam (excitation at 266 nm / 4.66 eV, < 2 ns pulse duration), and irradiation with pulsed electron beam of 270 KeV energy and 10 ns duration.. This energy is too low to produce lattice defects but high enough to produce electron – hole pairs. On the other hand the energy of the laser beam photons is too low to excite electron hole pairs but sufficient to excite intrinsic defects which act as luminescence centers. Luminescence intensity was measured using a photon counting head (Hamamatsu H8259) and a photon counting board (Fast Com Tec Communication Technology module P 7888-1E) with time resolution down to 2 ns. The experimental set up for luminescence intensity ensured that the differences of luminescence were due solely to the changes of the defect structure of the samples.

III. Results And Discusions

A. Structural Properties

XRD patterns and grain size distribution for both the nanopowder and nanostructured ceramics are shown in Fig.1. The monoclinic phase only was observed. The average grain size and grain size dispersion for MW ZrO_2 powder and HPLS ZrO_2 ceramics were 31 ± 4 nm and 27 ± 12 nm, respectively, (Fig. 1). The results of specific surface analysis ~ 40 m^2/g, are consistent with this grain size range.

The difference in grain size of the nanoparticles and the sintered ceramics may be an apparent effect and result from the high degree of microstrains in the ceramics. The ceramics were sintered at very high pressures and low temperatures, so that densification occurred without grain growth and diffusion. After sintering at high pressures the nano-sized grains become strained and this cause XRD peaks to broaden, which can be misinterpreted as grain refining. The method of XRD peak fine structure analysis of polidispersed powders (XRD-GSD) [15], as well as the Scherrer's method were developed for non-strained materials. Fig. 2 shows the morphology of both materials. The structure is uniform, indicating a mono-modal grain size distribution. There are fine particles agglomerated into larger aggregates of approximately 100 nm diameter. During synthesis of nanoparticles for photonic applications it is important to reach a high degree of crystallinity (i.e., low content of hydroxides, which are an intermediate product during the synthesis and may lead to luminescence quenching [15]. The good quality of the nanopowders is confirmed by their high density, ~ 5.9 g/cm^3.

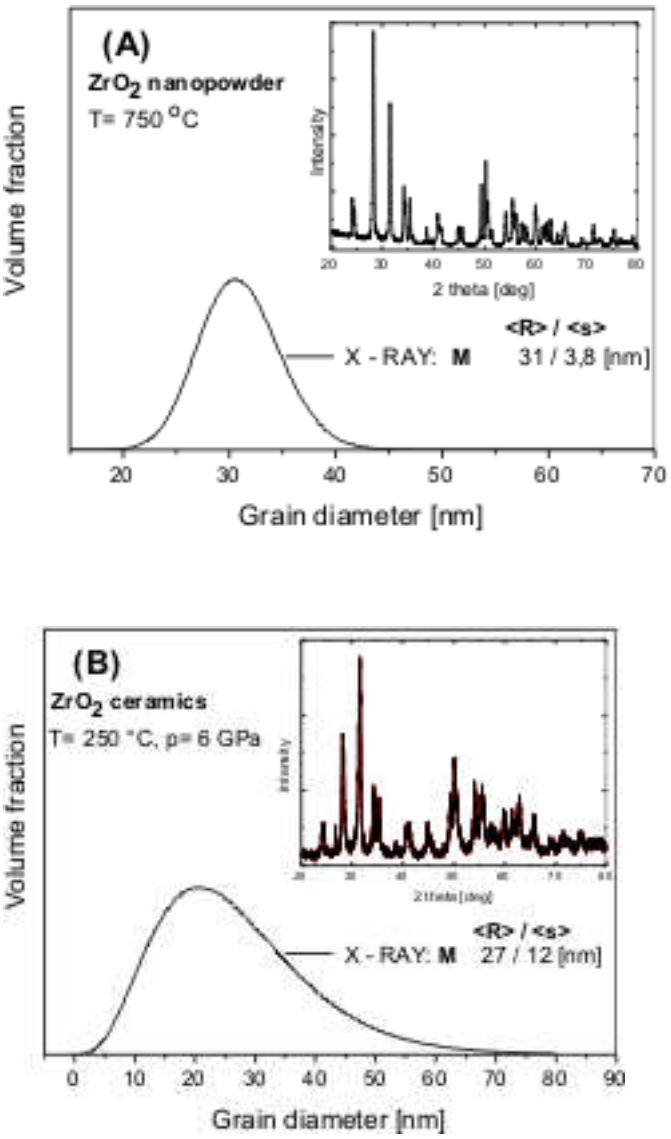

Figure. 1. GSD of the ZrO_2 nanopowder (A) and ZrO_2 nanostructured ceramics (B) obtained from analysis of the XRD data., <R> stands for average grain size, <s> – for dispersion of size. The peak at 26.7 is due to sample container used during sintering. The insets document the presence of only monoclinic phase in both samples.

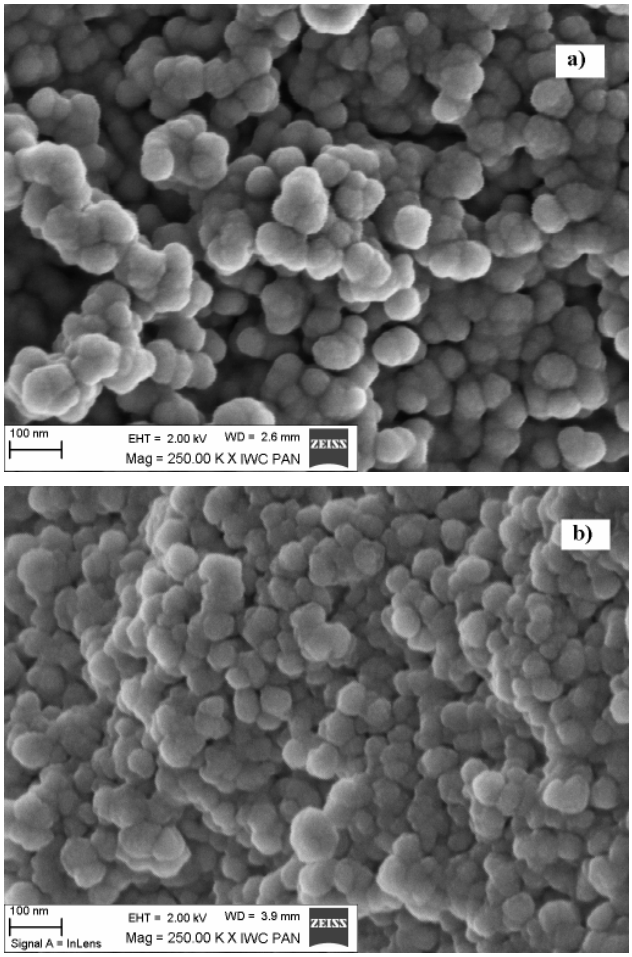

Figure 2. High resolution SEM images for a) ZrO_2 nanopowder (obtained by microwave driven hydrothermal synthesis, MW, and annealed at 750 °C for 30 min) and b) ZrO_2 nanostructured ceramics obtained from the MW ZrO_2 nanopowder (annealed at 750 °C for 15 min) under pressure 6 GPa at 250 ºC.

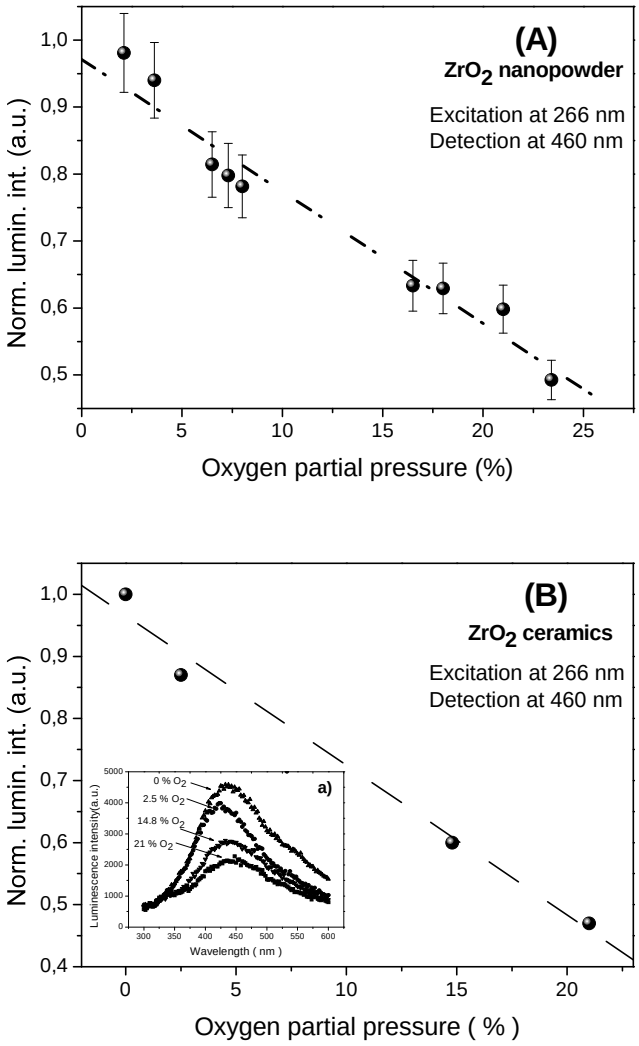

Figure 3. Luminescence intensity as a function of oxygen partial pressure for ZrO_2 nanopowders (A) and ZrO_2 nanoceramics (B) annealed in oxygen / nitrogen mixtures at 340 ºC. Luminescence was measured at RT under pulsed laser irradiation. The inset a) at (B) illustrates the example of luminescence spectra for ceramics.

B. Luminescence intensity dependence on oxygen content

Figure 3A shows that for samples annealed in mixtures of oxygen and nitrogen the luminescence intensity decreases proportionally to the increase of oxygen content. Also in the case of nanoceramics the luminescence signal increases as the oxygen pressure decreases (Fig. 3B). In ref [16] and in Fig. 3A it was shown that under monochromatic excitation by the laser beam the luminescence band shape is Gaussian and the position of the maximum of emission depends slightly on the excitation energy.

Figure 4 shows the oxygen partial pressure effect on the luminescence intensity measured using electron beam as excitation source. The intensity was measured at 2.8 eV/ 443 nm. It is clearly seen that contrary to laser beam excitation, the intensity increases as the oxygen pressure increases.

Real time luminescence investigations as a function of temperature with the use of electron beam excitation permitted to establish the optimum temperature for the sensor operation (Fig.5).

Figure 5 shows the effect of the following cycle of treatments on the luminescence intensity. First the measurement chamber was evacuated, the temperature was raised at a rate of 5 K/min and luminescence was continuously monitored. A continuous decrease of luminescence was observed. During cooling down (cycle 2) the luminescence level did not return to the initial value, what means that the defects that were created during annealing in vacuum did not disappear during cooling. However, when air was allowed in the experimental chamber, luminescence increased starting from 550K and reached a maximum at 620 K. This result confirms that efficient diffusion processes that lead to the creation or elimination of luminescence centers take place in the temperature range 550 – 650 K. This is therefore the optimum temperature range for operation of the sensor.

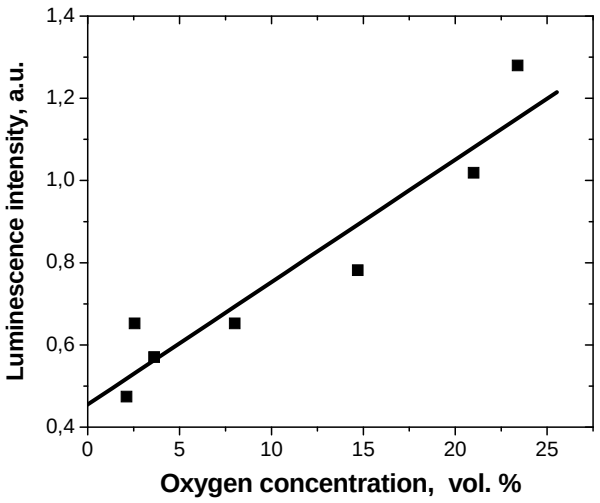

Figure 4. Effect of oxygen pressure on luminescence intensity at 2.8 eV / 443 nm for electron beam excitation.

.

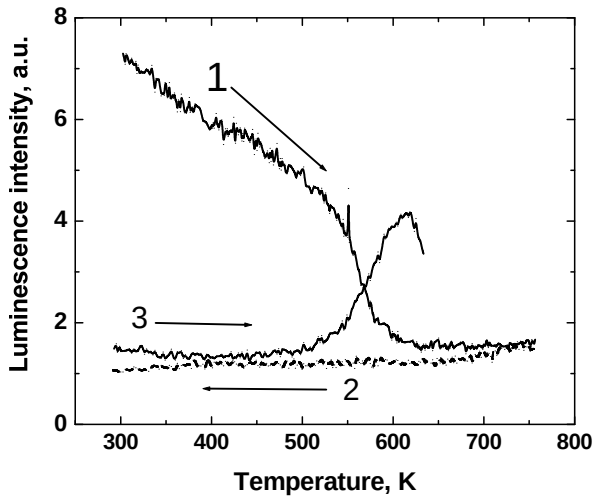

Figure 5. Real time measurements of zirconia nanopowders luminescence during electron beam excitation and during the following cycle of sample treatments. 1: heating in vacuum, 2" cooling in vacuum. 3; heating in air. Excitation energy 270 KeV, emission energy 2.8 eV/ 443 nm.

C. Mechanism of luminescence intensity dependence on oxygen pressure and the model of the luminescence centre in ZrO_2 nanoparticles

The present results are consistent with the idea, that the luminescence changes are connected with creation or elimination of oxygen vacancies close to the surface. However, the distribution and potential clustering of such vacancies within the nanoparticles lattice requires further studies. Recent positron annihilation studies indicate a presence of large free volumes (of the order of few atomic units, at least), open towards the nanocrystals surface [18]. Such a hypothetical structure change needs however further confirmation.

Annealing at low oxygen pressure leads to a higher oxygen vacancy concentration. Annealing at high oxygen pressure, on the contrary, to a decrease of vacancy concentration. Let us consider whether the vacancies themselves are luminescence centers or the luminescence centers are other defects that are induced by vacancies. To understand the luminescence mechanism it is crucial to consider the opposite effects of oxygen pressure on luminescence intensity for electron beam excitation (band to band) and for laser beam excitation (intra band).This effect can be explained assuming that the luminescence centers are not the vacancies but lattice site distortions caused by them [16,17]. For band to band excitation, an increase of vacancy concentrations leads to luminescence decrease because vacancies act as charge traps and provide non radiative recombination paths for the electron-hole pairs. On the other hand, for direct excitation of the luminescence centers within the band gap such a recombination mechanism is not possible, because the excited states are immobile (Fig. 6)..

This assumption is in agreement with induced transient absorption measurements – induced transient absorption decay time is more much longer than luminescence decay time [19]. This means that the trapped charges did not contribute in creation of luminescence centers excited states.

The above model explaining the difference in luminescence changes with oxygen pressure for the case of electron beam and laser beam excitation is explained schematically in Figure 6.

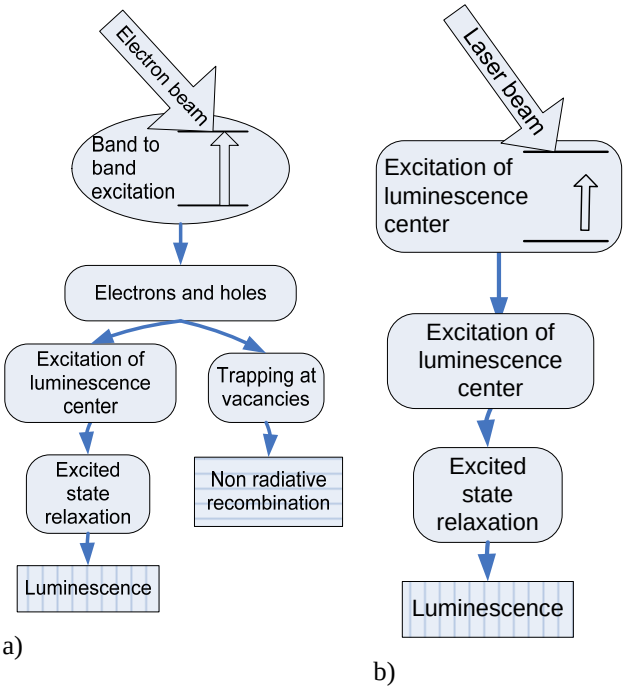

Figure 6. Schematic presentation of the recombination mechanism for a) electron beam excitation and creation of electron-hole pairs, b) laser beam excitation of intrinsic defects. In case a) vacancies provide non-radiative relaxation mechanisms.

The above presented results and model that explains them open the way for the use of nano-zirconia powders and ceramics in optical oxygen sensors operating at least in the temperature range 550 – 650 K. The optical signal can be measured after removing the material from the gas atmosphere or in real time using an appropriate optical system.

IV. Conclusion

ZrO_2 nanoparticles and nano-ceramic can be used as an optical oxygen pressure sensor with material operating optimally at 550 – 650K.

Under excitation by laser beam the intrinsic defects which are distorted lattice sites close to oxygen vacancies contribute to the observed increase of luminescence as oxygen pressure decreases.

Under excitation by electron beam the vacancies which are efficient traps for charge carriers suppress their recombination via light emission..

V. Acknowledgment

The authors thank Mr Mizeradzki for the SEM observations, Dr Gierlotka for XRD studies and Mr Zurek for high pressure sintering..

References

[1] R. C. Garvie, R. H. J. Hannink, and R. T. Pascoe, “Ceramic Steel?,” Nature, vol. 258, pp. 703, 1975.

[2] N. Nguyen, “Ceramic fuel cells,” J. Amer. Ceram. Soc, vol. 76, no. 3, pp. 563–588, 1993.

[3] A. V. Emmeline, G. N. Kuzmin, L. L. Basov, and N. Serpone, “Photoactivity and photoselectivity of a dielectric metal-oxide photocatalyst (ZrO_2) probed by the photoinduced reduction of oxygen and oxidation of hydrogen,” J. Photochem. Photobiol. A: Chem., vol. 174, pp. 214–221, 2005.

[4] H. Zhou, F. Li, B. He, J. Wang, and B. de Sun, “Air plasma sprayed thermal barrier coatings on titanium alloys substrates”, Surf. Coat. Technol., vol. 201, no. 16–17, pp. 7360-7367, 2007.

[5] J. D. Fidelus, S. Yatsunenko, M. Godlewski, W. Paszkowicz, E. Werner-Malento, and W. Łojkowski, “Relation between structural properties of Pr^{3+} -doped yttria-stabilized zirconia nanopowders and their luminescence efficiency,” Scripta Mater., vol. 61, pp. 415–418. 2009 (and references given there).

[6] E. Ivers-Tiffée, K. H. Härdtl, W. Menesklou, and J. Riegel, “Principles of solid state oxygen sensors for lean combustion gas control,” Electrochem. Acta, vol. 47 pp. 807–814, 2001 .

[7] M.Kirm, J.Aarik, and I.Sildos, “Thin films of HfO_2 and ZrO_2 as potential scintillators,” Nucl. Instrum. Meth. Phys. Res. A: vol. 537 issues1-2, pp.251–255, 2005

[8] N. G. Petrik, D. P. Tailor, and T. M. Orlando, “Laser-stimulated luminescence of yttria-stabilized cubic zirconia crystals,” J. Appl. Phys., vol. 85, No 9, pp. 6770–6776, 1999

[9] S. E. Paje and J. L. Lopis, “Disorder effects on the luminescence decay in yttria stabilized zirconia polycrystals,” J. Phys. D: Appl. Phys., vol. 29, pp. 442–445, 1996

[10] M. Anpo, T. Nomura, J. Kondo, K. Domen, K.-I. Maruya, and T. Onishi, Photoluminescence and FT-IR studies of the dissociative adsorption of H_2 on the active ZrO_2 catalyst and its role in the hydrogenation of CO,” Res. Chem. Intermediat. vol. 13, pp. 195–202, (1990)

[11] Q. Zhao, X. Wang, and T. Cai, “The study of surface properties of ZrO_2”, Appl. Surf. Sci., vol. 225, pp. 7-13, 2004

[12] J. Liang, X. Jiang, G. Liu, Zh. Dng, J. Zhuang, F. Li, J. Li, “Characterization and synthesis of pure ZrO_2 nanopowders via sonochemical method,” Mater. Res. Bull., vol. 38, pp.161–168, 2003.

[13] W. Łojkowski, D. Millers, J. Fidelus, L. Grigorjeva, A. Opalińska, U. Narkiewicz, and W. Stręk, “Zirconium dioxide luminescence oxygen sensor,” Patent Application PCT/Pl2006/000060, 01.09.2006, WO/2007/027116, 08.03.2007.

[14] J. D. Fidelus, W. Lojkowski, D. Millers D. K. Smits, L. Grigorjeva, R. R. Piticescu, “Zirconia-based nanomaterials for oxygen sensor - generation, characterisation and optical properties,” Solid State Phenom., vol. 128 , pp. 141–150, 2007.

[15] A. Opalinska, C. Leonelli, W. Lojkowski, R. Pielaszek, E. Grzanka, T. Chudoba, H. Matysiak, T. Wejrzanowski, and K. J. Kurzydlowski, “Effect of pressure on synthesis of Pr-doped zirconia powders produced by microwave-driven hydrothermal reaction,” J. Nanomate. 98769, pp. 1–8, 2006.

[16] K. Smits, L. Grigorjeva, W. Łojkowski, J. D. Fidelus, “Luminescence of oxygen related defects in zirconia nanocrystals,” Phys. Stat. Sol. (c) 4, No. 3, pp. 770–773, 2007/DOI 10.1002/pssc.200673850.

[17] K. Smits, D. Millers, L. Grigorjeva, J. D. Fidelus, W. Lojkowski, “Comparison of ZrO_2:Y nanocrystals and macroscopic single crystal luminescence,” J. Phys.: Conf. Ser.: vol. 93, pp. 012035, 2007.

[18] J. D. Fidelus, A. Karbowski, S. Mariazzi, R. S. Brusa, G. Karwasz, “Photoluminescence and positron annihilition studies of nanostructured ZrO_2”, Nukleonika, in press.

[19] K. Smits, L. Grigorjeva, D. Millers, J. D. Fidelus, W. Łojkowski, “Radiative decay of electronic excitations in ZrO_2 nanocrystals and macroscopic single crystals,” IEEE Trans. Nucl. Sci., vol. 55 (3), pp. 1523-1526, June 2008 [9th Internat. Conf. on Inorganic Scintillators and their Applications (SCINT 2007) Winston-Salem, NC, June 4-8, 2007].